Journal of
Applied Crystallography
ISSN 0021-8898

Received 16 August 2006
Accepted 15 December 2006

Complementary use of small-angle neutron scattering and dynamic light scattering studies for structure analysis and dynamics of polymer gels

Mitsuhiro Shibayama,[a,c]* Takeshi Karino,[a,c] Yusuke Domon[b] and Kohzo Ito[b,c]

[a]Institute for Solid State Physics, The University of Tokyo, 5-1-5 Kashiwanoha, Kashiwa, Chiba 277-8581 Japan, [b]Graduate School of Frontier Sciences, The University of Tokyo, 5-1-5 Kashiwanoha, Kashiwa, Chiba 277-8561 Japan, and [c]CREST, Japan Science and Technology Agency, 4-1-8 Honcho Kawaguchi Saitama, 332-0012 Japan. Correspondence e-mail: shibayama@issp.u-tokyo.ac.jp

Small-angle neutron scattering (SANS) and dynamic light scattering (DLS) have been complementarily employed in order to investigate the structure and dynamics of slide-ring (SR) gels, a class of novel polymer gels having advanced mechanical properties. SR gels consist of long flexible polymer chains and movable cross-links along the polymer chain. It is demonstrated that complementary use is necessary to explore the dynamics of SR gels. The sliding capability was verified by DLS and a low level of frozen inhomogeneities, originating from the sliding motion, was observed by SANS. DLS was also used to determine the sol–gel transition threshold and to decompose the scattering intensity into the dynamic fluctuating component and the frozen inhomogeneities. Both techniques clearly indicate the presence of the sliding mode in SR gels, which plays significant roles in the advanced mechanical and swelling properties.

1. Introduction

In the past five years, 'super gels' with remarkable mechanical properties have been reported, namely slide-ring (SR) gels (originally called topological gels) (Okumura & Ito, 2001), nanocomposite (NC) gels (Haraguchi & Takeshita, 2002), and double network (DN) gels (Gong *et al.*, 2003). For example, SR gels swell more than 30 000 times with respect to their dry state and the strength at breaking of an NC gel is more than 50 times as large as that of conventional gels. However, the origins of such properties were not well elucidated. It is needless to mention that a molecular-level investigation is necessary and scattering methods are powerful tools to explore the structure and dynamics of these super gels.

Polymer gels have a wide range of spatio-temporal heterogeneities ranging from nm to μm and ns to several s. Therefore, various scattering techniques covering these ranges, such as small-angle X-ray (SAXS) and/or small-angle neutron scattering (SANS) and light scattering, are necessary in order to characterize polymer gels. The structure and inhomogeneities of gels have been extensively investigated by these methods (Shibayama, 1998). Regarding dynamics, dynamic light scattering (DLS) and neutron spin echo spectroscopy (NSE) are complementary tools. In this paper, we discuss how these techniques are used in structure and dynamics studies of SR gels.

2. Theoretical background

2.1. Dynamics

The dynamics of complex fluids can be studied in either the frequency domain (ω domain) or the time domain (t domain). These domains are connected with the Wiener–Khinchin theorem,

$$I(q,\omega) = \frac{1}{2\pi}\int_{-\infty}^{\infty} \langle E_s^*(q,0)E_s(q,t)\rangle \exp(i\omega t)\,\mathrm{d}t. \quad (1)$$

q is the modulus of the scattering vector defined by $(4\pi/\lambda)\sin(\theta/2)$, where λ and θ are the wavelength and the scattering angle, respectively, and ω is the angular frequency. $E_s(q,t)$ is the scattering field at q and time t, and $E_s^*(q,t)$ is the complex conjugate of $E_s(q,t)$. In the case of NSE, the intermediate scattering function, $S(q,\omega)$ is directly obtained, from which the τ-dependent scattering intensity, $I_{\rm NSE}(q,\tau)$, is evaluated as

$$I_{\rm NSE}(q,\tau) \propto \int_{-\infty}^{\infty} S(q,\omega)\frac{1+\cos(\omega\tau)}{2}\,\mathrm{d}\omega \propto \exp(-Dq^2\tau). \quad (2)$$

Here τ is the decay time. The frequency shift by dynamical processes in the DLS regime, on the other hand, is very small with respect to the frequency of the light itself and is difficult to detect accurately. Hence, an approach in the t domain is commonly used. In this case, the scattering field correlation function, $g^{(1)}(q,\tau)$, is obtained by taking the photon correlation as given by

$$g^{(1)}(q,\tau) = \frac{\langle E_s^*(q,0)E_s(q,\tau)\rangle}{\langle |E_s(q,0)|^2\rangle} = \exp(-Dq^2\tau). \quad (3)$$

The experimentally observable quantity is the scattering intensity correlation function, $g^{(2)}(q,\tau)$. For ergodic media, $g^{(2)}(q,\tau)$ is obtained by

$$g^{(2)}(q,\tau) = 1 + \beta\sigma\exp(-2Dq^2\tau). \quad (4)$$

Here β is the coherence factor and σ is the initial amplitude of $g^{(2)}(q,\tau)$. σ is usually unity for ergodic media. Note that we assume here that the coherence factor is unity. However, in the case of

nonergodic media, such as polymer gels, $g^{(2)}(q,\tau)$ consists of two contributions, namely the dynamic fluctuations and the static inhomogeneities (Pusey & van Megen, 1989; Panyukov & Rabin, 1996). The latter is sample-position (p) dependent, and σ is much smaller than unity and p-dependent, *i.e.*, $\sigma = \sigma_p$. Hence, $g^{(2)}(q,\tau)$ is also p-dependent as given by

$$g_p^{(2)}(q,\tau) = 1 + X^2 g^{(1)}(q,\tau) + 2X(1-X)g^{(1)}(q,\tau) \simeq 1 + \sigma_p \exp(-2D_A q^2 \tau), \quad (5)$$

where D_A is the apparent diffusion coefficient obtained by the first cumulant of $g_p^{(2)}(q,\tau)$. The ratio X is defined as

$$X = \frac{\langle I_F \rangle_T}{\langle I \rangle_{T,p}}. \quad (6)$$

Here, $\langle \ldots \rangle_T$ means the time average. $\langle I \rangle_T$ is the scattering intensity and $\langle I_F \rangle_T$ is its fluctuating component. Decomposition of $\langle I \rangle_T$ can be uniquely carried out by using the plot (Shibayama *et al.*, 1996)

$$\frac{\langle I \rangle_{T,p}}{D_A} = \frac{2}{D}\langle I \rangle_{T,p} - \frac{\langle I_F \rangle_T}{D}. \quad (7)$$

Here, D is the collective diffusion coefficient as firstly defined by Tanaka (Tanaka *et al.*, 1973), which is related to the correlation length of polymer gels, ξ, by (de Gennes, 1979)

$$\xi = \frac{kT}{6\pi\eta D}. \quad (8)$$

Note that this equation is the same as the Stokes–Einstein equation for dilute polymer solutions and for dispersed systems with the hydrodynamic radius R_h,

$$R_h = \frac{kT}{6\pi\eta D}. \quad (9)$$

2.2. Static structure factor

In most cases, the static structure factor for polymer gels can be approximated by a sum of Lorentz (Ornstein–Zernike type) functions and squared-Lorentz functions,

$$I(q) = \frac{I_L(0)}{1+\xi^2 q^2} + \frac{I_{SL}(0)}{(1+\Xi^2 q^2)^2}, \quad (10)$$

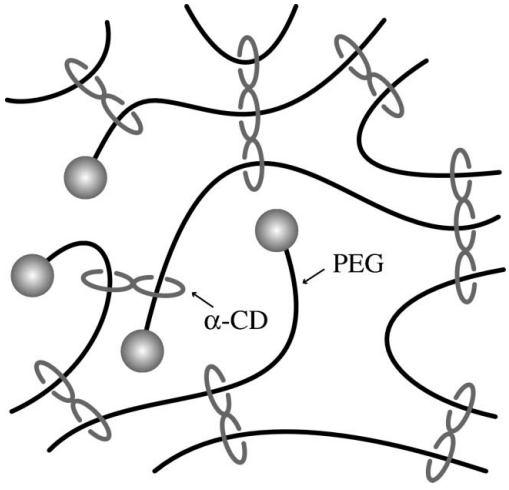

Figure 1
Schematic model of an SR gel. End-capped polyrotaxane chains are cross-linked *via* a coupling reaction of CD molecules to form an infinite network, *i.e.*, an SR gel.

where Ξ is the characteristic length of frozen inhomogeneities (Shibayama, 1998). When Ξ is the same as ξ, the equation is reduced to that proposed by Onuki (1992) for describing inhomogeneities in deformed gels. However, in general, Ξ is not necessarily the same as ξ. The presence of Ξ is the characteristic feature of gels which possess spatial or cross-link inhomogeneities.

3. Experimental

3.1. Samples

Polyrotaxane was prepared from poly(ethylene glycol) (PEG) and α-cyclodextrin (α-CD) in water at 353 K. The molecular weight of PEG was 3.50×10^4 g mol^{-1}. Fig. 1 shows a schematic illustration of an SR gel. Polyrotaxane chains, consisting of PEG chains and α-CD molecules, are cross-linked by a coupling reaction of α-CD molecules to form an infinite network. Note that α-CD cross-links are expected to slide freely along the PEG chain. End-capping of polyrotaxane occurred by chemical reaction with 2,4-dinitrofluorobenzene. The filling ratio of α-CD with respect to PEG was 27%. Gelation of the polyrotaxane was made in a 1 *N* NaOH solution at 278 K. Cyanuric chloride, dissolved in 1 *N* NaOH (aq), was mixed with the solution to initiate the cross-linking reaction. Thus, SR gels were prepared. The details of SR gel preparation are described elsewhere (Okumura & Ito, 2001; Karino *et al.*, 2004).

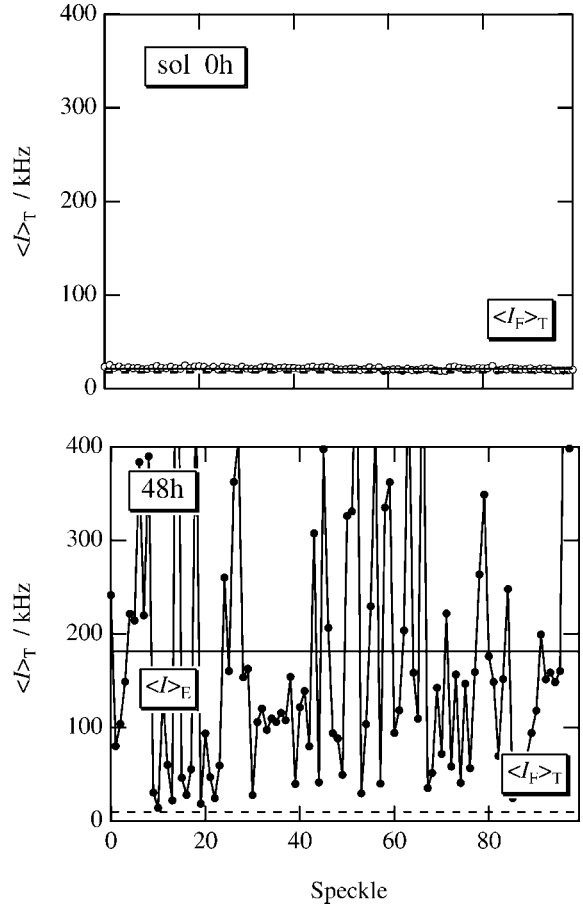

Figure 2
Speckle patterns of an SR solution (top) and an SR gel (bottom).

3.2. DLS

DLS experiments were carried out on a static/dynamic compact goniometer (SLS/DLS-5000), ALV, Langen, Germany. An He–Ne laser at 22 mW (λ = 632.8 nm) was used as the incident beam at a fixed angle of 90°. Time-intensity correlation functions, $g^{(2)}(q, \tau)$, were measured for α-CD solutions, polyrotaxane, and SR gels, at 298 K for 30 s, followed by a general-purpose constrained regulation method for continuous distributions (CONTIN) analysis in order to obtain the decay rate distribution function, $G(\Gamma)$, where τ and Γ are the decay time and the decay rate, respectively. The value of β was better than 0.98.

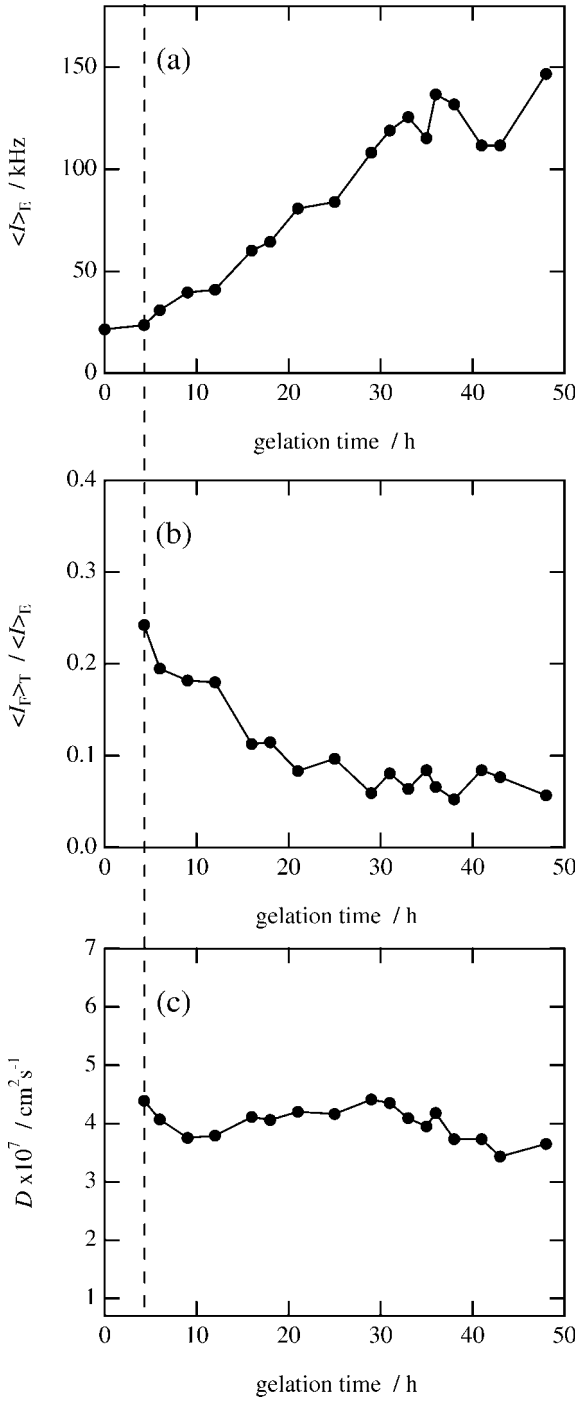

Figure 3
Gelation time dependence of (*a*) $\langle I \rangle_E$, (*b*) $\langle I_F \rangle_T / \langle I \rangle_E$, and (*c*) D.

3.3. SANS

SANS experiments were carried out at the SANS-U spectrometer (Institute for Solid State Physics, The University of Tokyo, at Tokai, Japan), which is installed in the Guide Hall of the JRR-3M Research Reactor (20 MW), Japan Atomic Energy Agency, Tokai (λ = 7.0 Å and λ distribution 10%). The sample-to-camera distance was 4 m. The SANS data were corrected and rescaled to the absolute intensities. The performance and the procedure of data reduction are described elsewhere (Okabe *et al.*, 2005; Shibayama *et al.*, 2005).

4. Results

It is known that speckle patterns are exclusively observed in light scattering due to nonergodicity when a highly coherent laser is used as an incident beam (Pusey & van Megen, 1989; Joosten *et al.*, 1991; Shibayama, 1998). Fig. 2 shows examples of light speckle patterns observed at θ = 90° for a polyrotaxane solution (top) before and

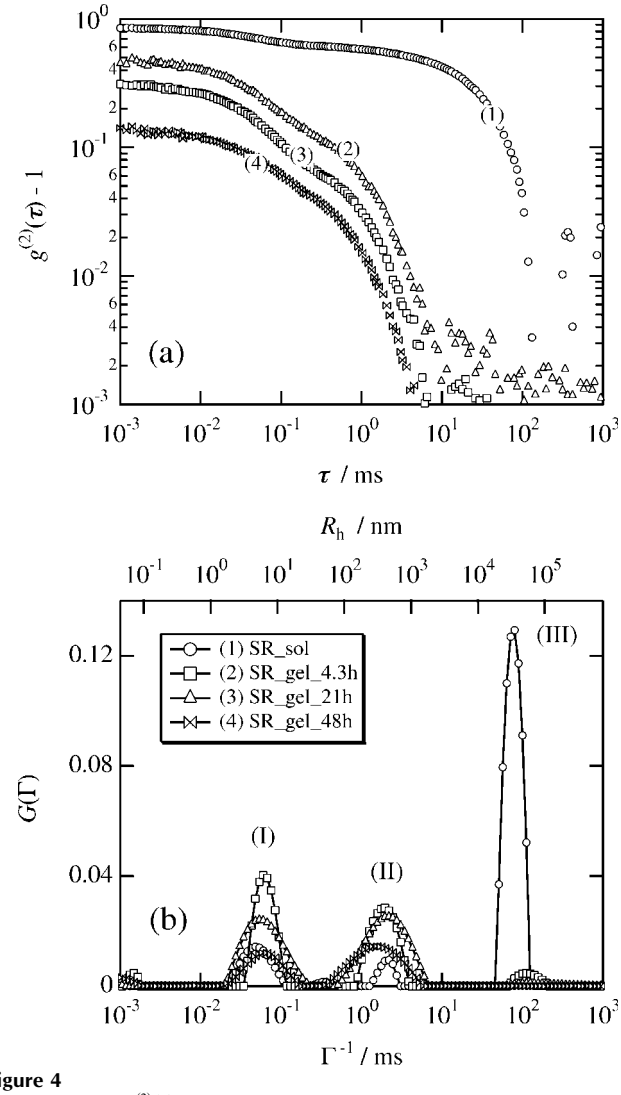

Figure 4
(*a*) Variations of $g^{(2)}(\tau)$ during gelation of an SR gel. (*b*) The corresponding $G(\Gamma)$ functions. Modes (I), (II), and (III) correspond to the collective diffusion, sliding motion, and polymer diffusion modes, respectively.

(bottom) after completion of gelation. Gelation was made by a coupling reaction of α-CD with cyanuric chloride at 293 K as described above. The dashed and solid horizontal lines show $\langle I_F \rangle_T$ and the ensemble-average scattering intensity, $\langle I \rangle_E$, respectively. Investigations of speckle patterns during the gelation process allowed us to determine the gelation threshold as *ca.* 4.3 h in this particular case.

Fig. 3 shows the gelation time dependence of (*a*) $\langle I \rangle_E$, (*b*) the ratio of dynamic fluctuations to frozen inhomogeneities, $\langle I_F \rangle_T / \langle I \rangle_E$, and (*c*) D, for an SR gel observed at $\theta = 90°$. The vertical dashed line indicates the gelation threshold. As shown in the figure, $\langle I \rangle_E$ and $\langle I_F \rangle_T / \langle I \rangle_E$ increases and decreases rather gradually with gelation time, respectively. On the other hand, D remains rather constant at *ca.* 4×10^{-7} cm^2 s^{-1} after gelation.

Fig. 4 shows (*a*) $g^{(2)}(\tau) - 1$ and (*b*) $G(\Gamma)$ for an SR gel during the gelation process. Before the gelation threshold, polyrotaxane solution has a slow mode around $\tau = 10^2$ ms. However, at the gelation threshold, the shoulder in $g^{(2)}(\tau) - 1$ shifts toward the faster decay time [(1) to (2)]. This is followed by suppression of σ from unity [(2) to (3) and (4)]. This systematic change is more clearly observed in $G(\Gamma)$ as shown in Fig. 4(*b*). The SR solution has a predominant slow mode designated by (III) and small peaks marked by (I) and (II). On the other hand, the resultant SR gel has an intermediate mode (II) in between and the mode (III) disappears. This phenomenon is explained as follows. Mode (III) corresponds to the translational motion of the polyrotaxane chain, which disappears on cross-linking. Mode (II) is assigned to be a 'sliding' mode since it is amplified by cross-linking (Zhao *et al.*, 2005). Although the physical meaning of the magnitude of the characteristic decay time, *ca.* 2 to 3 ms, is not clear at this stage, it may indicate a dragging motion of CD rings along PEG chains.

The static structures of SR gels were investigated with SANS. Fig. 5 shows SANS intensity functions of SR gels in NaOD. The polymer concentration was 10 wt%. The cross-linker concentrations, C_X, are shown by weight percentage with respect to the gel. The SANS intensity function, $I(q)$, for polyrotaxane solution (coded as C_X = 0 wt%) is well represented by a Lorentz function [equation (10) with $I_{SL}(0) = 0$] with $\xi = 43.7$ Å. Interestingly, by introducing cross-links, ξ decreased up to $C_X = 2$ wt%, and then increases with increasing C_X. More interestingly, as shown in Fig. 6, two-dimensional SANS intensity patterns for deformed SR gels in dimethylsulfoxide showed normal butterfly patterns and a normal-to-abnormal butterfly-pattern transition was observed by increasing C_X from 0.75 to 2.0 wt%, indicating immobilization of sliding cross-links (Karino *et al.*, 2005). The presence of the sliding motion detected by DLS as well as the normal-to-abnormal butterfly transition observed in SANS clearly demonstrate that the microscopic structures of SR gels are very different from those of conventional chemical gels made by radical copolymerization of monomer and cross-linker.

5. Discussion

Cross-linking sometimes enhances concentration fluctuations as frozen inhomogeneities and suppresses dynamic concentration fluctuations (Shibayama, 1998; Ikkai & Shibayama, 2005). Cross-linking enlarges the spatial correlation if the polymer concentration C is low, *i.e.*, $C < C^*$, where C^* is the chain overlap concentration (de Gennes, 1979). On the other hand, it screens the spatial correlation for $C > C^*$, while the connectivity correlation diverges (Shibayama *et al.*, 2000). In addition to these experimental results reported in the literature, the above experimental results disclosed in this work indicate that a wide space–time range is necessary to fully understand the structure and dynamics of gels. This is because polymer gels have hierarchical structure introduced by cross-linking.

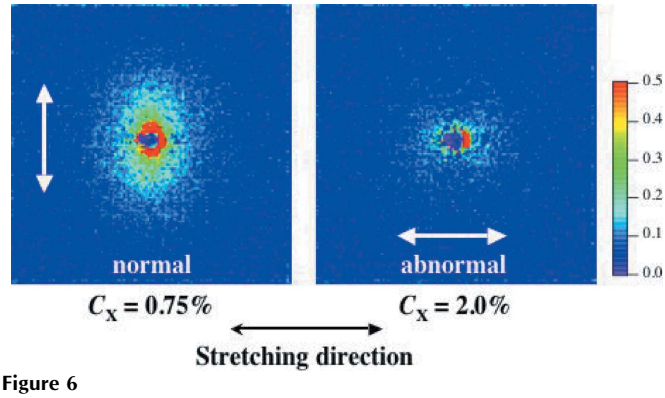

Figure 6
SANS intensity functions of deformed SR gels with C_X = 0.7 (left) and 2.0 wt% (right). The stretching ratio was 1.75. An normal (left) to abnormal butterfly-pattern (right) transition was observed by increasing C_X, indicating immobilization of movable cross-links.

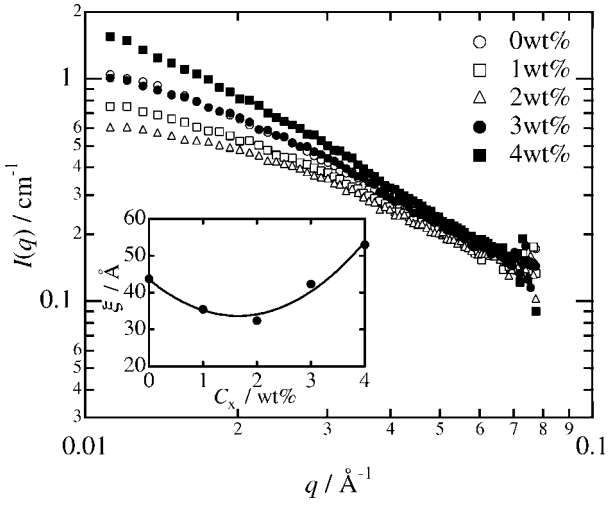

Figure 5
SANS intensity functions for SR gels with C_X = 0, 1, 2, 3, and 4 wt%. The inset shows the C_X dependence of ξ.

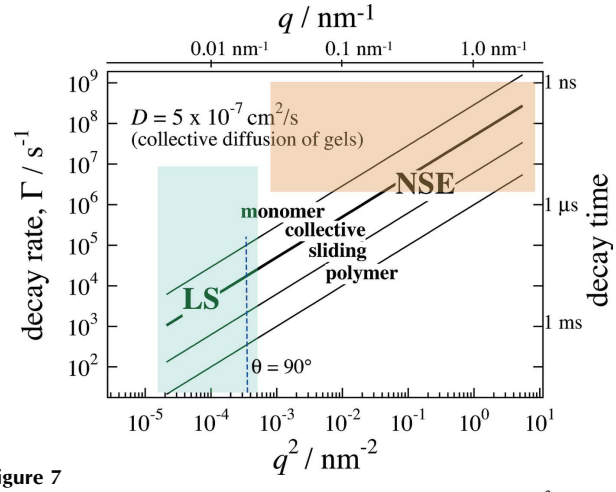

Figure 7
Spatio-temporal relationship for the various modes in SR gels. The q^2 dependence of the four modes, *i.e.*, monomer diffusion, collective diffusion, the sliding motion, and polymer diffusion, are plotted.

In Fig. 7 is plotted the characteristic decay rates (Γ) as a function of the modulus of the scattering vector squared (q^2). The slope, *i.e.*, $D = \Gamma/q^2$ gives the diffusion coefficient for monomer diffusion, collective diffusion, sliding motion, and polymer diffusion in semi-dilute solutions. The shaded areas denote the DLS and NSE regimes for typical setups. All of the modes assigned in Fig. 4 can be, in principle, observed by both DLS and NSE. However, this map clearly shows that DLS seems to be the most suitable means for structure/dynamics investigation of polymer gels. In the case of DLS, it is advantageous to employ the high coherence of lasers. Light scattering from gels contains speckles, which are sensitive to inhomogeneities. As a result, *distribution analyses* of DLS data employing inverse Laplace transformation, *time-resolved DLS*, and *ensemble-average DLS* allow us to decompose decay modes, to determine a gelation threshold (Shibayama & Norisuye, 2002), and to decompose concentration fluctuations into dynamic fluctuations and frozen inhomogeneities (Shibayama, 1998), respectively. The dynamic aspects and deformation mechanisms of polymer gels are discussed elsewhere by DLS and SANS (Zhao *et al.*, 2005; Karino *et al.*, 2005).

It should be borne in mind, however, that the territory of NSE is rapidly growing in both time and q ranges. Since the advantage of neutron scattering is its short wavelength suitable for investigation of dynamics in the polymer coil dimension, NSE covers the missing region and allows one to study Rouse and Zimm modes in polymer gels. As a matter of fact, preliminary NSE experiments on SR gels recently carried out at the National Institute of Standards and Technology indicated a crossover from Rouse to Zimm modes.

References

Gennes, P. G. de (1979). *Scaling Concepts in Polymer Physics*. Ithaca: Cornell University Press.

Gong, J. P., Katsuyama, Y., Kurokawa, T. & Osada, Y. (2003). *Adv. Mater.* **15**, 1155–1158.

Haraguchi, K. & Takeshita, T. (2002). *Adv. Mater.* **14**, 1120–1124.

Ikkai, F. & Shibayama, M. (2005). *J. Polym. Sci. B Polym. Phys. Ed.* **43**, 617–628.

Joosten, J. G. H., McCarthy, J. L. & Pusey, P. N. (1991). *Macromolecules*, **24**, 6690–6599.

Karino, T., Okumura, Y., Ito, K. & Shibayama, M. (2004). *Macromolecules*, **37**, 6117–6182.

Karino, T., Okumura, Y., Zhao, C., Kataoka, T., Ito, K. & Shibayama, M. (2005). *Macromolecules*, **38**, 6161–6167.

Okabe, S., Nagao, M., Karino, T., Watanabe, S., Adachi, T., Shimizu, H. & Shibayama, M. (2005). *J. Appl. Cryst.* **38**, 1035–1037.

Okumura, Y. & Ito, K. (2001). *Adv. Mater.* **13**, 485–487.

Onuki, A. (1992). *J. Phys. II France*, **2**, 45–61.

Panyukov, S. & Rabin, Y. (1996). *Phys. Rep.* **269**, 1–132.

Pusey, P. N. & van Megen, W. (1989). *Physica A*, **157**, 705–741.

Shibayama, M. (1998). *Macromol. Chem. Phys.* **199**, 1–30.

Shibayama, M., Fujikawa, Y. & Nomura, S. (1996). *Macromolecules*, **29**, 6535–6540.

Shibayama, M., Nagao, M., Okabe, S. & Karino, T. (2005). *J. Phys. Soc. Jpn*, **74**, 2728–2736.

Shibayama, M. & Norisuye, T. (2002). *Bull. Chem. Soc. Jpn*, **75**, 641–659.

Shibayama, M., Tsujimoto, M. & Ikkai, F. (2000). *Macromolecules*, **33**, 7868–7876.

Tanaka, T., Hocker, L. O. & Benedek, G. B. (1973). *J. Chem. Phys.* **59**, 5151–5159.

Zhao, C., Domon, Y., Okumura, Y., Okabe, S., Shibayama, M. & Ito, K. (2005). *J. Phys. Condens. Matter*, **17**, S2841–S2846.